Science of the Total Environment 858 (2023) 159662

Contents lists available at ScienceDirect

Science of the Total Environment

journal homepage: www.elsevier.com/locate/scitotenv

Trace metals distribution between the surface waters of the Gulf of Cadiz and the Alboran Sea

M. Andrea Orihuela-García [a,b,*], Marina Bolado-Penagos [a], Iria Sala [c,d], Antonio Tovar-Sánchez [e], Carlos M. García [d], Miguel Bruno [a], Fidel Echevarría [d], Irene Laiz [a]

[a] Departamento de Física Aplicada, Facultad de Ciencias del Mar y Ambientales, Instituto Universitario de Investigación Marina (INMAR), Campus de Excelencia Internacional/Global del Mar (CEI·MAR), Universidad de Cádiz, Puerto Real, Cadiz, Spain
[b] Departamento de Ciencias de la Tierra, Centro Nacional de Supercomputación (CNS), Barcelona, Spain
[c] Department of Mathematics and Statistics, University of Strathclyde, G1 1XH Glasgow, United Kingdom
[d] Departamento de Biología, Facultad de Ciencias del Mar y Ambientales, Instituto Universitario de Investigación Marina (INMAR), Campus de Excelencia Internacional/Global del Mar (CEI·MAR), Universidad de Cádiz, Puerto Real, Cadiz, Spain
[e] Departamento de Ecología y Gestión Costera, Instituto de Ciencias Marinas de Andalucía ICMAN-CSIC, Puerto Real, Cadiz, Spain

HIGHLIGHTS

- Trace metals' concentrations diminish offshore and eastwards.
- Vertical mixing hinders trace metals' flow from the Gulf of Cadiz.
- Easterly wind and tidal mixing may hamper trace metals' eastward transport.
- Retention areas with long residence time are related to higher metal concentrations.

GRAPHICAL ABSTRACT

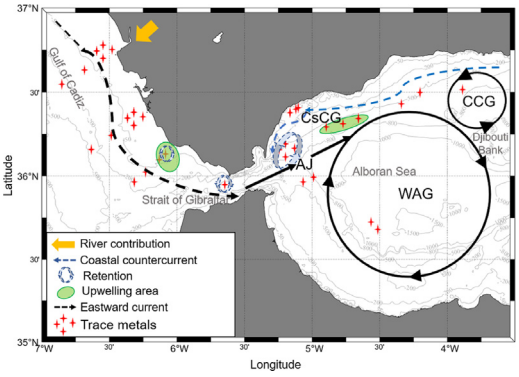

ARTICLE INFO

Guest Editor: Julian Blasco

Keywords:
Trace metals
Easterly wind
Surface current
Alboran Sea
Gulf of Cadiz
Strait of Gibraltar

ABSTRACT

This study was conducted to address the changes in the surface distribution of trace metals (cobalt, copper, iron, cadmium, nickel, zinc, lead and molybdenum) as they are advected from the Gulf of Cadiz to the Alboran Sea, through the Strait of Gibraltar (south Iberian Peninsula), regions of great ecosystemic importance. Trace metals concentrations were measured in samples collected during two oceanographic cruises, together with the main factors affecting their spatial distribution and temporal variability (i.e., wind and surface currents). Several rivers, the main source of trace metals in this region, flow into the Gulf of Cadiz which is connected with the Alboran Sea through the Strait of Gibraltar by the general circulation pattern. The surface circulation pattern leads to an offshore-eastward gradient that is highly influenced by wind variability. An increase in vertical turbulence induced by the winds or the tidal cycle causes the dilution of trace metals' concentration by mixing rich-metal superficial waters with poor-metal subsurface waters. Additionally, along the eastward displacement of surface waters, several water retention zones have been described (Trafalgar, Camarinal, the Coastal Cyclonic Gyre) that imply an increase in trace metals concentration close to the coast. In addition, our results suggest that the coastal edges of the Strait of Gibraltar also act as a source of certain metals to the Alboran Sea, probably due to the industries in the proximity areas.

* Corresponding author at: Departamento de Ciencias de la Tierra, Centro Nacional de Supercomputación (CNS), Barcelona, Spain.
E-mail address: andrea.orihuela@bsc.es (M.A. Orihuela-García).

http://dx.doi.org/10.1016/j.scitotenv.2022.159662
Received 30 March 2022; Received in revised form 17 October 2022; Accepted 19 October 2022
Available online 24 October 2022

1. Introduction

Trace metals (e.g., cobalt (Co), copper (Cu), iron (Fe), molybdenum (Mo), zinc (Zn), nickel (Ni), and vanadium (V)) play an important role in the ocean's biogeochemical cycles, but at certain concentrations, they might be toxic, (e.g., cadmium (Cd), Cu, lead (Pb)), both for marine organisms and for humans (e.g., Morel and Price, 2003). Nevertheless, trace metals are essential for the development of life (e.g., Sunda, 1989). For instance, Fe and Cu are fundamental for electron transport in photosynthesis, respiration, and nitrogen fixation (among other functions), Co is necessary to produce vitamin B_{12}, Zn is essential for nucleic acid replication and transcription synthesis, and Ni participates in the hydrolysis of urea and, together with Cd, is also present in different functions as hydration and dehydration of carbon dioxide (Twining and Baines, 2013).

River discharges are often considered the main source of trace metals in the ocean, (Henderson et al., 2007; Gaillardet et al., 2014). However, the origin of trace metals in the marine environment is also related to the deposition of aerosols (van Geen and Boyle, 1990) submarine groundwater discharge (e.g., Tovar-Sánchez et al., 2014), diffuse sources at continental margins or from the deep sea (Blasco et al., 2000), hydrothermal (Geibert, 2018) and ice sources (Tovar-Sánchez et al., 2010), or anthropogenic sources. Anthropogenic sources are related to agriculture (e.g., Kidd et al., 2007; Micó et al., 2006), acid mine drainage (e.g., Hierro et al., 2014), modifications in the rivers suspended loads, drilling or industrial activities (Blasco et al., 2000; Cotté-Krief et al., 2000), or oil spills (Zhang et al., 2020), among others. These and other sources of trace metals from the different ocean boundaries have been recently compiled by the GEOTRACES international program (https://www.geotraces.org) (Geibert, 2018). Once a trace metal reaches the ocean, it starts being dispersed and diluted. For dissolved trace metals, which will be the focus of this study, advection and mixing processes are the main transport mechanisms (Hatje et al., 2018; Tovar-Sánchez et al., 2018). Advection can take place due to oceanic or tidal currents and submesoscale processes (e.g., upwelling and downwelling, eddies). Mixing can result from wind or waves stirring, but also from concentration gradients (Hatje et al., 2018; Tovar-Sánchez et al., 2018).

The Gulf of Cadiz (GoC, hereinafter) – southwestern Iberian Peninsula – shelf waters were considered to have substantially higher concentrations of dissolved Cd, Cu, and Zn than other coastal regions worldwide (van Geen et al., 1991). The rivers Tinto, Odiel, Guadalquivir, and Guadiana (see Fig. 1a) represent the main source of trace metals on the GoC continental shelf (e.g., van Geen et al., 1991; Boyle et al., 1985; González-Ortegón et al., 2019). These rivers drain the Iberian Pyrite Belt and mining activities have heavily contaminated them (Nieto et al., 2006) enhancing metal concentrations at the GoC (e.g., Periáñez, 2009). In addition, there is a marine dump near the Guadalquivir estuary, where dredged material is deposited periodically (Donázar-Aramendía et al., 2018).

Due to these high metal concentrations and the fact that the GoC shelf waters could export trace metals to the adjacent Alboran Sea (Boyle et al., 1985; van Geen et al., 1988) several studies have focused not only on the origin and fluxes of metals onto the GoC continental shelf (e.g., Braungardt et al., 2003; Olías et al., 2006; González-Ortegón et al.,

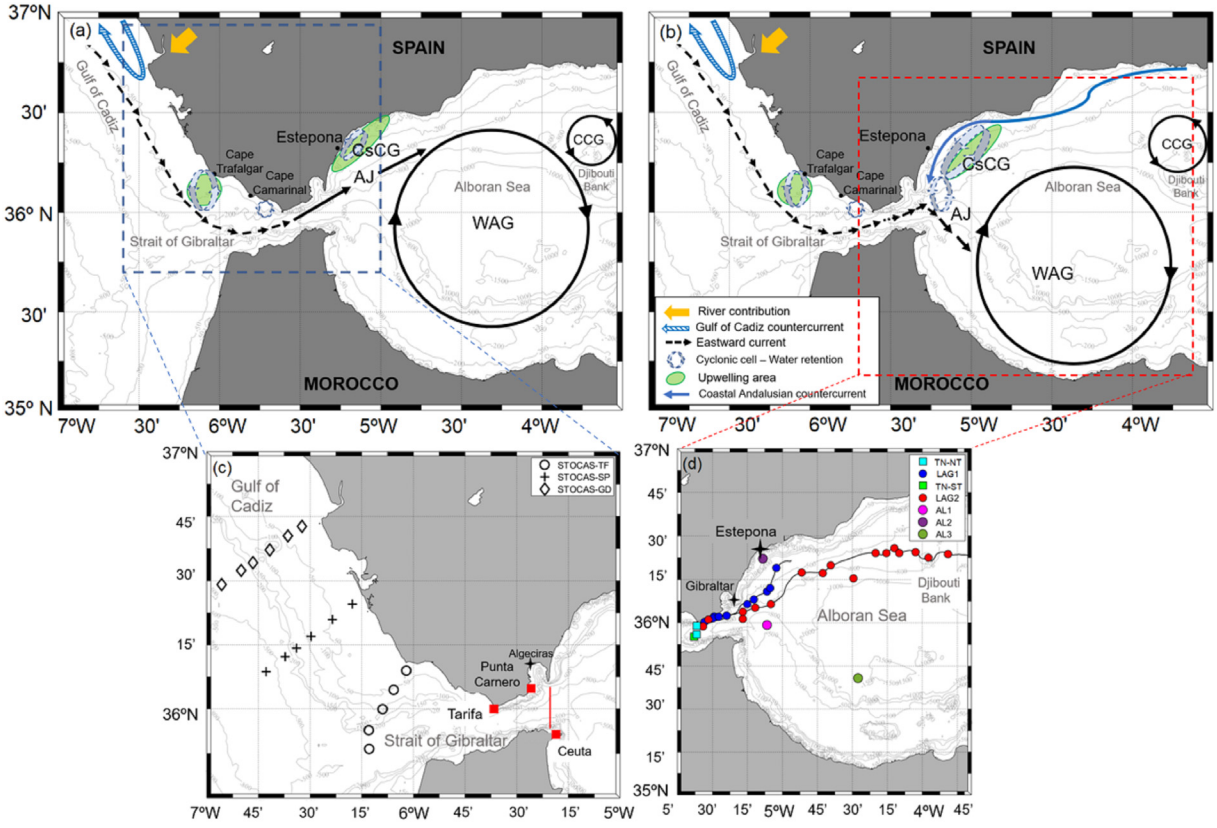

Fig. 1. Map of the study area focused on the Gulf of Cadiz – Strait of Gibraltar – Alboran Sea. (a) Conceptual diagram of the main surface circulation pattern under westerlies and (b) easterlies. The yellow arrow indicates river contribution. Green arrows indicate the upwelling areas. The blue dashed arrow indicates the Gulf of Cadiz coastal countercurrent. The thin blue line indicates the coastal Andalusian countercurrent. The dashed blue square in (a) encloses the (c) location of the sampling stations during the STOCA cruise: Guadalquivir (GD; diamonds), Sancti Petri (SP; crosses) and Trafalgar (TF; circles). Red squares indicate the position of the High-Frequency radar antennas. The longitudinal red line indicates where the surface current velocity and direction from the radar dataset were retrieved. The dashed red square in (b) encloses the (d) sampling stations during the MEGAN cruise: Tarifa Narrow stations during neap (TN-NT, light blue squares) and spring (TN-ST, green squares) tides, Lagrangian stations during neap (LAG1, blue dots) and spring (LAG2, red dots) tides, and Alboran stations (AL1, pink dots; AL2, purple dots; AL3, green dots). AJ: Atlantic Jet; WAG: Western Anticyclonic Gyre; CsCG: CoaStal Cyclonic Gyre; CCG: Central Cyclonic Gyre.

2019) but also on their spatial distribution and transport (e.g., Elbaz-Poulichet et al., 2001; Beckers et al., 2007; Periáñez, 2009; Laiz et al., 2020). Laiz et al. (2020) found that once the dissolved trace metals reach the GoC continental shelf, they are transported along the inner shelf by surface currents and, depending on the circulation pattern, can reach the Alboran Sea (to the east), the Portuguese shelf (to the west), or even be retained near their source.

However, to the best of our knowledge, none of these studies has addressed the role played by the different hydrodynamic processes involved in the surface circulation pattern from the GoC to the Alboran Sea through the Strait of Gibraltar (hereinafter, SoG) in the distribution of trace metals using in-situ data. Therefore, the objectives of this study are: 1) to analyse the trace metals distribution variability across the GoC - SoG - Alboran Sea using in-situ data sampled during different oceanographic campaigns, and 2) to relate the variability of sub- and mesoscale structures, and the hydrodynamics of the study area, to the observed metal concentrations and distribution.

2. Oceanographic context

The GoC is characterised by a complex circulation (e.g., Sánchez and Relvas, 2003). During summer, it presents a generalised anticyclonic pattern (Sánchez and Relvas, 2003; Criado-Aldeanueva et al., 2006) that might change to cyclonic during late autumn-early winter (Mauritzen et al., 2001; Criado-Aldeanueva et al., 2006, 2009). More recent studies have demonstrated that this anticyclonic-cyclonic shift recurrently occurs throughout the year (Garel et al., 2016). When the circulation over the eastern shelf is cyclonic, a westward-flowing coastal current is observed (dashed blue arrow in Fig. 1a and b). The onset of this current, also known as coastal counter-current, might respond to different forcing mechanisms, including easterly winds, the relaxation of westerlies or an alongshore pressure gradient (Mauritzen et al., 2001; Relvas and Barton, 2002; García-Lafuente et al., 2006; Sánchez et al., 2006; Garel et al., 2016; De Oliveira Júnior et al., 2021). This counter-current generally occupies the eastern shelf but, under easterly winds, it may reach the western shelf or even continue flowing northward along the western Portuguese shelf (e.g., Relvas and Barton, 2002; Laiz et al., 2020).

The Atlantic inflow (also known as Atlantic Jet, AJ) is the primary driver of the Alboran Sea surface circulation (e.g., Bormans and Garrett, 1989; Renault et al., 2012). The AJ feeds the quasi-permanent Western Alboran Gyre (WAG) and a Coastal Cyclonic Gyre (CsCG) that arises close to the Estepona coast associated with the upwelling of nutrient-rich waters (Fig. 1a) (Sarhan et al., 2000; Macías et al., 2008). This system is highly influenced by atmospheric forcing (e.g., García-Lafuente et al., 2002; Bolado-Penagos et al., 2021). The AJ flows through the SoG with an average speed of $\sim$1 m s^{-1} and enters the Alboran Sea with a predominantly northeast orientation. When westerly winds prevail (Fig. 1a), i.e., under low atmospheric pressure at the western Mediterranean Sea, its intensity increases while its northeast orientation is reinforced (e.g., Macías et al., 2016). In this case, the CsCG is constrained to the coast enhancing the upwelling of nutrient-rich waters and leading to high chlorophyll-*a* (Chl-*a*) concentrations (Fig. 1a) (Sarhan et al., 2000; Macías et al., 2008). Conversely, when easterly winds predominate, coinciding with high pressure at the western Mediterranean Sea (e.g., Macías et al., 2016; Bolado-Penagos et al., 2021), the intensity of the AJ is reduced and it veers southwards adopting the so-called coastal mode (black arrow in Fig. 1b, e.g., Macías et al., 2008). Under these conditions, the system formed between the AJ and the WAG can become destabilized (e.g., Viúdez et al., 1998) and the AJ can even reverse its direction (García-Lafuente et al., 2002). As a result, the upwelling that characterises the Estepona coast, associated with the CsCG, is less intense, wider, and moves offshore (Fig. 1b) (Sarhan et al., 2000; Macías et al., 2008; Bolado-Penagos et al., 2021). In addition, the presence of a coastal countercurrent flowing along the Andalusian border until Gibraltar (Reyes, 2015; Chioua et al., 2017; Bolado-Penagos et al., 2021), and its interaction with the Atlantic flow, forms a cyclonic cell at the easternmost part of the SoG (Soto-Navarro et al., 2016; Chioua et al., 2017; Bolado-Penagos et al., 2021).

In the SoG, the tidal current interacts with the sharp topography. This interaction is notable in Cape Trafalgar and, although less intense, in Camarinal Sill (Tarifa, Fig. 1). As a result, the development of a cyclonic gyre to the east of these two regions, associated with a quasi-permanent upwelling, increases the retention of the upwelled waters (Vargas-Yáñez et al., 2002; Bruno et al., 2013; Sala et al., 2018; Bolado-Penagos et al., 2020; Sala, 2021). Under westerly wind conditions, the connection SoG – Alboran Sea is favoured, and the upwelled waters are slowly transported towards the Alboran Sea along the coastal fringe. In contrast, under intense and persistent easterly wind conditions, this connection is interrupted, and the residence time of the water mass increases (Bolado-Penagos et al., 2020).

3. Data and methodology

3.1. In-situ sampling stations

This work examines the trace metals concentration data collected as part of the Spanish National project MEGOCA (*Study of the trace metal content in the Gulf of Cadiz: Influence of the Guadiana, Tinto, Odiel and Guadalquivir rivers*), from two different oceanographic campaigns: STOCA (*Time Series Oceanographic Data Campaign in the Gulf of Cadiz*) and MEGAN (*Mesoscale and submesoscale processes in the Strait of Gibraltar*: *The Trafalgar-Alboran connection*).

The STOCA campaign took place in the GoC between 15th and 17th September 2015. A total of 17 sampling stations were defined along three transects perpendicular to the coast in front of the Guadalquivir River (GD), Sancti Petri (SP), and Cape Trafalgar (TF) (see Fig. 1c).

The MEGAN campaign was carried out between 21st September and 11th October 2015 within the SoG and the western Alboran Sea. This cruise comprised different sampling phases (see Fig. 1d): the Tarifa Narrows during neap (TN-NT; 5 stations) and spring (TN-ST; 6 stations) tides; the Lagrangian phase during neap (LAG1; 11 stations) and spring (LAG2; 17 stations) tides; and the Alboran daily cycles (AL1, AL2, AL3; 15 stations). During the TN phases, different water samples were taken at the same points within the SoG in the course of a day. During the Lagrangian phases, water samples were collected by following the path of two Lagrangian buoys launched on neap and spring tides (Sala et al., 2022) conditions. Finally, during the Alboran daily cycles, water samples were collected in three different areas; one influenced by the AJ (AL1), the other at the Estepona coast (AL2) and the last at the centre of the WAG (AL3); the sampling was carried out on a 6-hourly basis for one day.

3.2. Trace metals analysis

Sea surface water (1–5 m depth) for trace metals analysis (Cd, Co, Cu, Fe, Mo, Ni, Pb, and Zn) was collected at each sampling station using a Teflon towfish system deployed from the research vessel (González-Ortegón et al., 2019). The water was pumped for 10 min in a class-100 HEPA laminar flow hood through acid-cleaned Teflon tubing that was coupled to C flex tubing. For this purpose, a Teflon diaphragm pump (Sandpiper cole-Palmer) was used. The samples were then filtered online through an acid-washed 0.22 μm polypropylene Calyx capsule filter and collected into 500 mL acid-washed LDPE bottles. All the samples were acidified on board to pH < 2 with ultrapure grade Hydrochloric acid (Merck) and kept in storage for at least 1 month before extraction. Finally, the samples were pre-concentrated using a liquid-organic extraction method (Tovar-Sánchez, 2012) and analysed using inductively coupled plasma-mass spectrometry (ICP-MS, iCAP Thermo). The accuracy of the pre-concentration method and analysis for each campaign was established using Nearshore Seawater Reference Material for Trace Metals (CASS 4, NRCCNRC) with a range of recoveries from 92 % for Co to 106 % for Cd. Table S1 summarises the compiled and analysed data.

3.3. Ancillary meteo-oceanographic variables

The following meteorological and oceanographic variables were analysed for the whole study area and period to examine their influence on the variability and distribution of the metal concentrations:

Hourly *wind data* (m s^{-1}) (at 10-m height) were acquired from the ERA5 meteorological reanalysis (https://www.ecmwf.int/).

Hourly *surface current velocity data* (m s^{-1}) were obtained from the SAMPA (*Sistema Autónomo de Medición, Predicción y Alerta*) model (https://www.puertos.es/es-es/Paginas/AFondo/Sampa.aspx). Additionally, to determine the entry angle of the AJ, surface current velocity data were also acquired from the *Puertos del Estado* High-Frequency (HF) radar antennas system, along a transect at the easternmost exit of the SoG (5.40°W and 35.90–36.10°N; red longitudinal transect in Fig. 1c).

Daily satellite images of *surface Chl-a concentration*, to identify the presence of upwellings, were retrieved from the Copernicus Marine Service (https://marine.copernicus.eu/).

More detailed information about data and methodology can be found in the supplementary material.

4. Results

4.1. Meteo-oceanographic conditions

The GoC was sampled during westerly wind conditions (Fig. 2a), which favoured an eastward surface circulation (Fig. 3a).

The SoG was sampled during neap tides (TN-NT stations and the first 6 stations of the LAG1) under very weak westerlies (0.00–0.50 m s^{-1}, 24th September, Fig. 2a) and during spring tides (TN-ST and the first 2 stations of the LAG2) under weak easterlies (−2.00–0.00 m s^{-1}, 1st to 3rd October) preceded by an event of strong easterly winds (−8.00 and − 4.00 m s^{-1}, 27th September until 1st October). During the spring tide period, a change in the AJ direction was observed at the easternmost part of the SoG, reaching an entering angle of 180° on 29th September (Fig. 2b).

The western Alboran Sea was sampled during neap tides (LAG1) under weak easterlies (−1.00–0.00 m s^{-1}) and during spring tides (LAG2) under increasing and variable westerlies (Fig. 2a). Moreover, the AL* daily cycles were carried out under weak westerly winds (1.00–3.00 m s^{-1}, 8th to 11th October, Fig. 2a). During this period, the AJ already recovered its characteristic entering angle (around 90°–135°) (Fig. 2b).

Fig. 3 shows the surface current velocity obtained from the SAMPA model along the study area during the different sampling periods. During the STOCA (GoC), TN-NT and LAG1 samplings, the AJ was characterised by a speed of ~1.40 m s^{-1} and entered the Alboran Sea with an angle of 135° (Fig. 2b), coupled with the WAG (Fig. 3 a-c). The CsCG, associated with the Estepona upwelling, can be observed at its typical location during westerly winds (white squares in Fig. 3a and c). As previously observed in Fig. 2b, the AJ began to flow southeastward from 30th September onwards (during MEGAN spring tide sampling), with a current speed between 0.60 and 1.00 m s^{-1}, adopting the coastal mode (Fig. 3d and e). As a result, a cyclonic gyre appeared at the easternmost exit of the SoG (red circles east of the SoG in Figs. 3d-f). Finally, during the AL* sampling, the AJ increased its intensity up to 1.50 m s^{-1} and entered the Alboran Sea east/northeast oriented (Fig. 3f).

Fig. 4 shows the Chl-*a* concentration surface distribution in the study area during the sampling period. During the STOCA cruise, a high Chl-*a* concentration (~ 5 mg m^{-3}, Fig. 4a) was observed at the GoC coastal margin. In the TF region, a tongue of relatively high Chl-*a* concentration (1.00–3.00 mg m^{-3}) was presently associated with the quasi-permanent upwelling that characterises this region. However, the highest concentration (~ 6 mg m^{-3}) for the whole study area was registered along the northwestern coast of the Alboran Sea, associated with CsCG (Figs. 4a and 3a). In the following days, a progressive decrease in the Chl-*a* concentration took place in the whole area. The Chl-*a* concentration varied between 2.00 and 3.00 mg m^{-3} at the stations sampled on the northwestern coast of the Alboran Sea during neap tide (Fig. 4b) and was lower during spring tide, ranging between 0.50 and 1.00 mg m^{-3} (Fig. 4c). During the AL* sampling, the coast of Estepona (AL2, Fig. 4d) showed a slight increase in the Chl-*a* concentration (1.00–2.00 mg m^{-3}) compared to the previous days, with an offshore decreasing gradient, reaching concentration values of 0.10–0.20 mg m^{-3} at the centre of the WAG (Fig. 4d).

4.2. Trace metals concentration and distribution

4.2.1. Gulf of Cadiz

In the GoC, the trace metals concentration (disregarding Pb and Mo) presented an offshore and eastward decreasing gradient (Fig. 5). Thus, the highest values of Co (0.75 nM), Cu (16.81 nM), Cd (0.35 nM), and Zn (26.51 nM) were observed at the coastal stations of the GD transect (Figs. 5 a-f, Table S1 for more details). For example, the coastal Zn value in this transect is 8 times higher than the TF transect coastal value. Meanwhile, the highest concentration of Pb (0.67 nM) was observed in the TF transect coastal station (Fig. 5g, Table S1), representing the largest

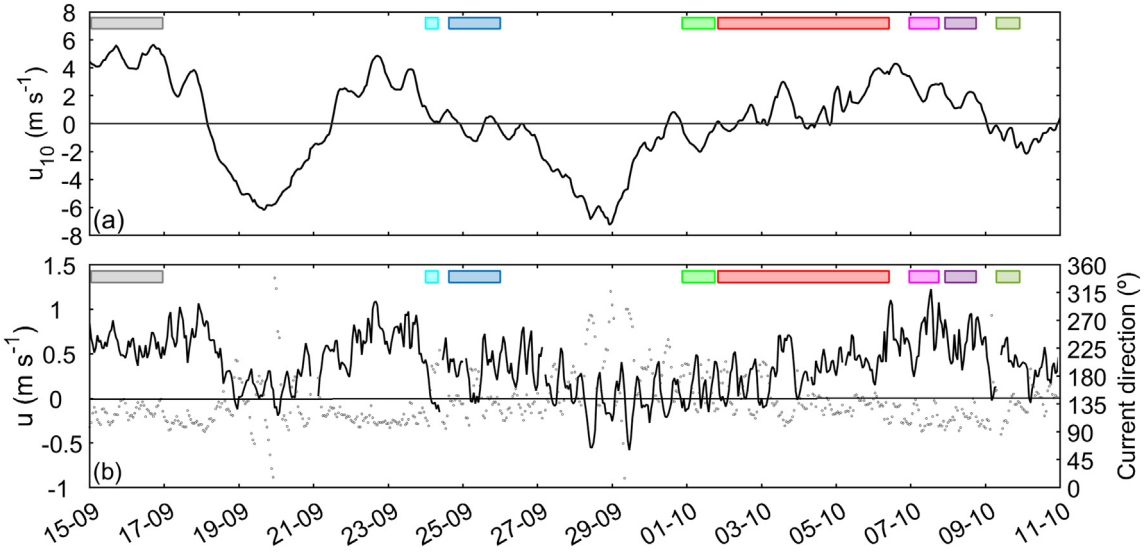

Fig. 2. Temporal variability of (a) hourly zonal wind component at 10-m height (u_{10}, m s^{-1}), and (b) High-Frequency radar derived zonal surface current speed (u, m s^{-1}; black line) and direction (polar coordination system; grey points) averaged over the transect located at the easternmost side of the Strait of Gibraltar (red line in Fig. 1b). Positive/negative values indicate that wind and current flow eastward/westward towards the Alboran Sea/Gulf of Cadiz, respectively. Coloured rectangles indicate the water sampling periods: STOCA in grey, TN-NT in light blue, LAG1 in blue, TN-ST in light green, LAG2 in red, AL1 in pink, AL2 in purple and AL3 in green.

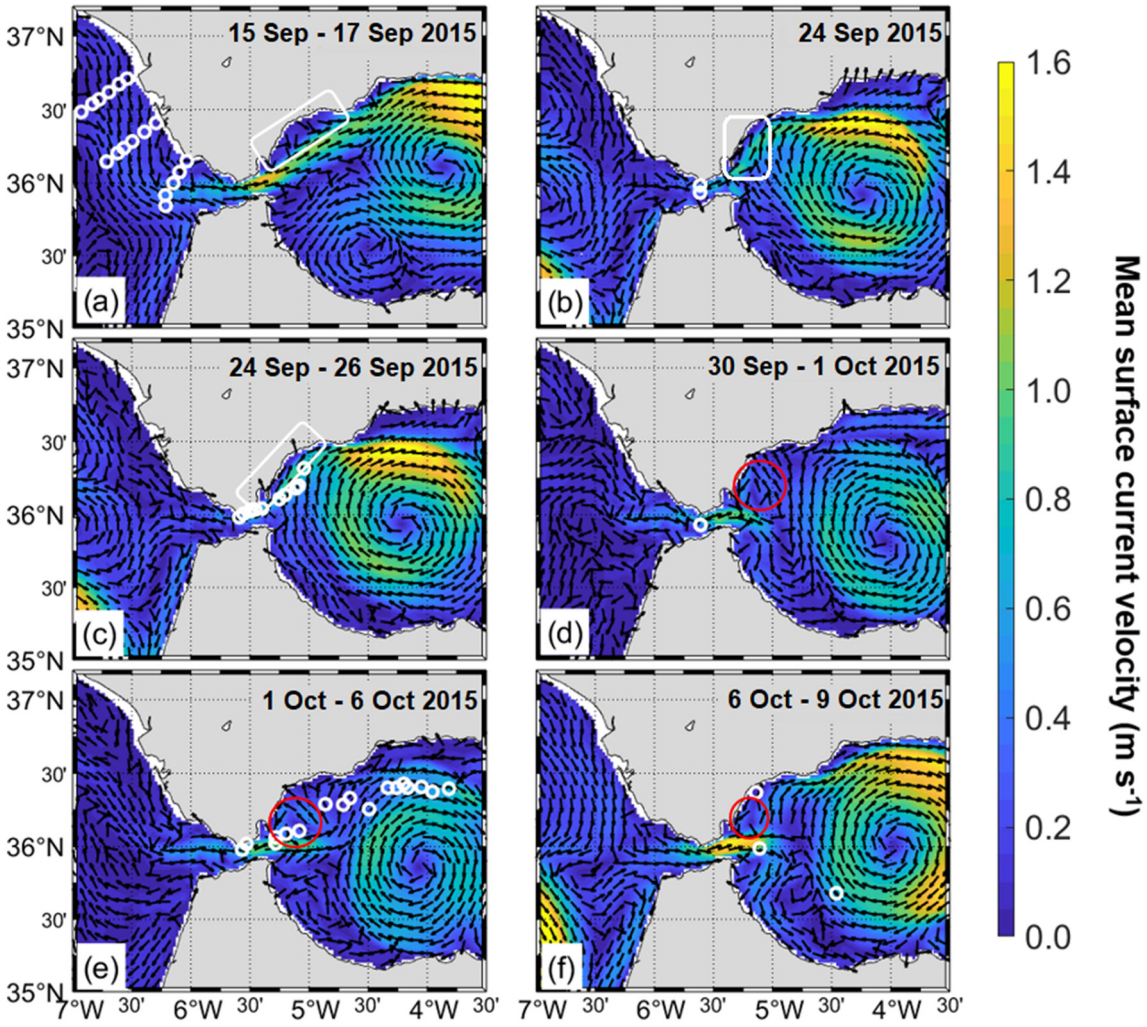

Fig. 3. Mean surface current velocity (m s^{-1}) from SAMPA model computed for the different sampling periods: (a) STOCA, (b) TN-NT, (c) LAG1, (d) TN-ST, (e) LAG2, and (f) AL* (includes AL2, AL1, and AL3, from north to south). White rectangles indicate the coastal upwelling and the coastal cyclonic gyre (CsCG) location. Red circles indicate the position of the cyclonic gyre at the easternmost exit of the SoG.

concentration of this metal among both cruises. Mo did not show a clear pattern of variability in this basin (Fig. 5h, Table 1).

4.2.2. Strait of Gibraltar

Disregarding Mo and Ni that showed similar mean values in the GoC and the SoG, the mean metal concentrations within the SoG (TN stations and the firsts stations of the Lagrangian phases) were lower than in the GoC (Fig. 6, Table 1) during both neap and spring tides. Compared with the GoC, Fe showed the lowest difference (~ 1.08 times lower), and Zn showed the highest (~ 4.78 times higher).

The mean values for Co, Cu, Fe, Cd, and Zn decreased between 1.10 and 1.83 times from neap to spring tides, while Pb decreased 3.03 times. During neap tides, a decreasing gradient was observed from the coastal edge to the centre of the channel, where the metal concentrations were ~1.5 times lower (left panels in Fig. 6, Table S1). In the case of Cu, Fe, and Zn, their concentrations were twice as high at the coastal stations than at the centre of the channel. During spring tides, the trace metals concentrations were also higher at the coastal edge than at the centre of the channel, but the variability was smaller (coastal concentrations were ~1.1 times higher than those at the centre of the channel) (right panels in Fig. 6). When comparing the trace metals concentrations obtained at the coastal edge during neap and spring tides, the former always showed larger values by a factor of 3 (Pb), 1.5 (Cu, Fe, Zn), 1.1 (Cd, Co), or 1.05 (Ni, Mo).

4.2.3. Alboran Sea

The Lagrangian phases (Fig. 6) allowed us to simultaneously study the longitudinal and temporal variability of trace metals as the AJ enters the Alboran Sea. However, for the sake of simplicity, we will describe the longitudinal variability. Meanwhile, the Alboran daily cycles (Fig. 7), allowed us to analyse the coastal-offshore variability.

Along the western Alboran Sea, the concentration values observed for Co, Cu, Cd, and Pb were two times lower than those recorded in the GoC, while Zn showed 5.2 times lower values (Fig. 7, Tables 1 and S1). The Fe concentration was ~2.08 times higher than the one observed along the GoC. Mo and Ni showed similar ranges of variability (Table 1). Compared to the SoG, the mean values of Cd, Cu, Mo, and Zn showed a slight decrease, ranging between 1.03 and 1.15 times lower, while Pb showed the highest decrease (1.88 times lower). Fe, Co, and Ni concentrations were, respectively, ~2.5, 1.5 and 1.20 times higher in the Alboran Sea than in the SoG.

Comparing the tidal legs, the concentrations of all metals were generally higher during neap tides than during spring tides (Table S1), with a constant of proportionality ranging between 1.05 (Mo, Ni), 1.30 (Co, Cu, Cd, Zn), 1.60 (Fe), and 2.00 (Pb). However, a west-to-east gradient was not observed. During neap tides (LAG1), the highest concentrations for all the trace metals were found at the beginning of the buoy trajectory, i.e., at the westernmost region of the northwestern Alboran Sea, while the lowest concentrations were observed at the easternmost stations, i.e., at the end of the buoy trajectory

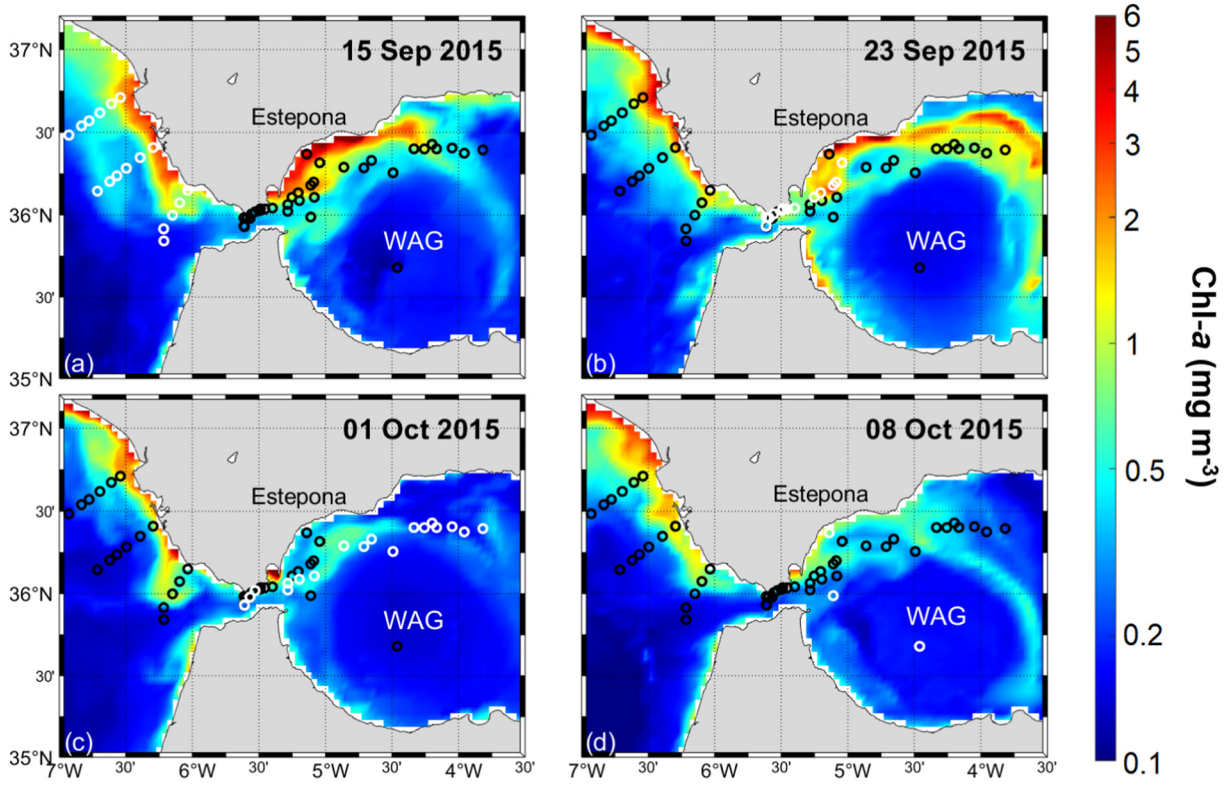

Fig. 4. Surface Chlorophyll-*a* concentration (Chl-*a*, mg m^{-3}) during the different sampling periods: (a) STOCA, September 15th, 2015; (b) MEGAN neap tide legs (TN-NT and LAG1), September 23rd, 2015; (c) MEGAN spring tide legs (TN-ST and LAG2), October 1st, 2015; and (d) MEGAN Alboran daily cycles (AL), October 8th, 2015.

(left-hand side panels in Fig. 6, Table S1). Whereas during spring tides (LAG2), the highest concentrations of Cu (4.40 nM), Fe (4.05 nM), and Mo (119.51 nM) were found next to the easternmost exit of the SoG, i.e., at the beginning of the buoy trajectory. Besides, the highest values of Ni (3.69 nM), Pb (0.22 nM), and Zn (1.70 nM) were found at the end of the buoy journey, near Djibouti Bank (right-hand side panels in Fig. 6).

Contrary to the GoC, a decreasing offshore gradient was not clearly observed for all the trace metals (Fig. S1). The highest concentrations of Fe (60.12 nM) and Ni (4.13 nM) were registered at the coastal station (AL2, Fig. 7a, c and e) and represented the largest values among both cruises (STOCA and MEGAN). In fact, the Fe concentration was ~40 times higher than the lowest concentration in the Alboran Sea (1.36 nM, recorded at

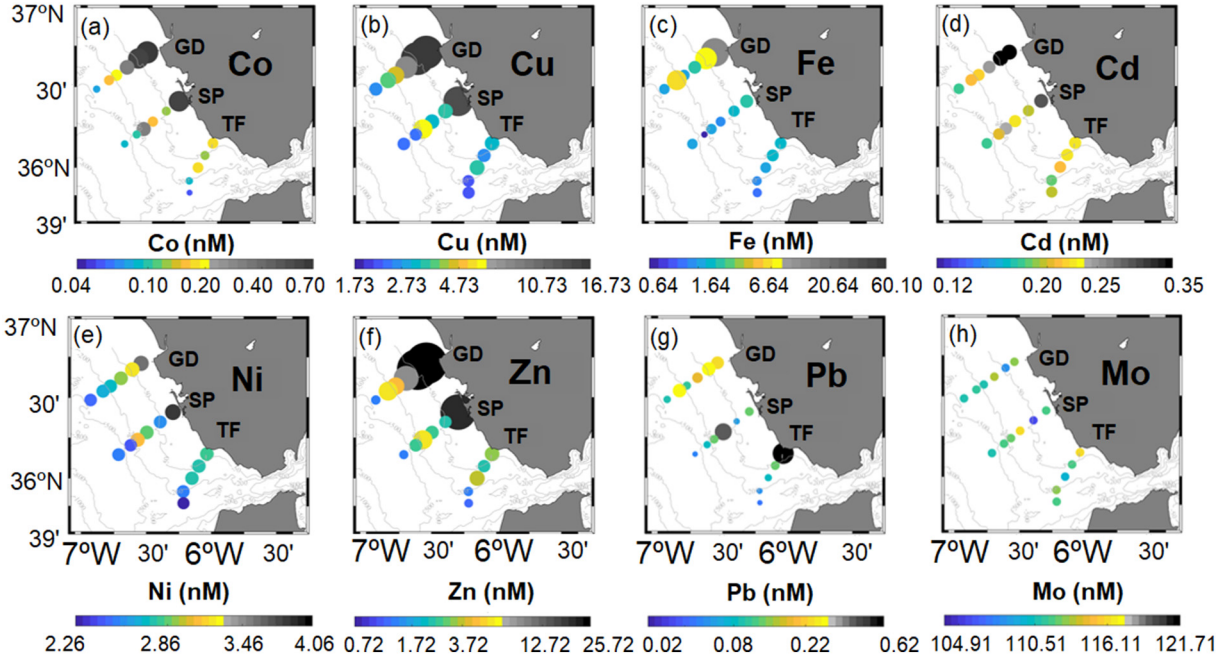

Fig. 5. Trace metals concentration (nM) at STOCA sampling stations along the Guadalquivir (GD), Sancti Petri (SP) and Trafalgar (TF) transects: (a) cobalt (Co), (b) copper (Cu), (c) iron (Fe), (d) cadmium (Cd), (e) nickel (Ni), (f) zinc (Zn), (g) lead (Pb), and (h) molybdenum (Mo). The size of the circles is proportional to the concentration of each metal. Please note the different ranges of scales between subplots.

Table 1
Range of trace metals concentration in the three different regions of study: the Gulf of Cadiz (GoC), the Strait of Gibraltar (SoG) and the Alboran Sea.

	Cd (nM)	Co (nM)	Cu (nM)	Fe (nM)	Mo (nM)	Ni (nM)	Pb (nM)	Zn (nM)
GoC	(0.17–0.35)	(0.05–0.75)	(2.12–16.81)	(0.64–12.29)	(105.70–115.99)	(2.26–3.84)	(0.05–0.67)	(1.20–26.52)
SoG	(0.13–0.21)	(0.04–0.16)	(2.28–6.42)	(1.09–4.52)	(109.16–122.05)	(2.44–3.23)	(0.04–0.47)	(0.00–3.78)
Alboran Sea	(0.12–0.20)	(0.06–0.26)	(1.73–6.10)	(1.36–60.12)	(102.11–120.14)	(2.61–4.13)	(0.02–0.22)	(0.72–3.71)

the centre of the WAG) and ~ 100 times higher than the minimum value observed in both cruises (0.64 nM in the SP transect). Except for Mo, Zn, and Fe, the lowest trace metals concentration and the lowest variability, between measurements at the same station, were observed at the AL1 station (influenced by the AJ, Fig. S1). Mo showed the lowest concentration at AL2 (102.11 nM, Fig. 7h, Table S1), while the minimum values for Fe (1.53 nM) and Zn (0.77 nM) were observed at AL3 (Fig. 7). Nevertheless, at AL3 (the centre of the WAG), high values of Cu, Zn and Mo (6.10 nM, 3.71 nM and 120.15 nM, respectively, Fig. 7b, f and h) were also reported.

Overall, most metals showed higher concentrations at the Coast than at the Jet, as shown in Fig. S1. In this sense, the mean concentrations of Co, Ni, Zn, and Pb were 1.50 times higher at the coast than at the rest of the stations, those of Cd and Cu were 1.10 times higher, and that of Fe was 5.57 times higher. On the contrary, Mo showed 1.05 times higher concentrations at the Jet. Finally, also the coastal stations showed higher values than the WAG. For example, the concentration of Fe was 10 times higher at the coast and those of Co, Ni, Zn, and Pb were 1.30 times higher (Fig. S1), with Zn showing the largest variability among measurements. However, while Cd presented similar concentrations in both regions, Mo and Cu showed 1.05 and 1.23-times higher values in the WAG than at the coast, respectively (Fig. S1).

5. Discussion

5.1. Gulf of Cadiz

The average values of Co, Cu, Cd and Zn in the Gulf of Cadiz were the highest for the whole study (Fig. 8, Table S1). Considering that the main rivers flowing into the GoC drain the Iberian Pyrite Belt (Leistel et al., 1997) and that they are subject to numerous anthropogenic activities, these trace metals high values were probably associated with river discharges (mainly the Guadalquivir River, as indicated by González-Ortegón et al., 2019). In fact, six days before the STOCA campaign a peak was observed in the Guadalquivir River runoff (see Fig. S2), the nutrient input of which would favour an increase in the phytoplankton community, and therefore in the Chl-*a* concentration along the GoC continental shelf (Fig. 4a). Furthermore, the sampled water mass corresponded to the Spanish Shelf Water (salinity = 36.00–36.25 and temperature = 20.00 °C–22.00 °C) (Fig. S3a), which is characteristically rich in trace metals (van Geen et al., 1988; Laiz et al., 2020). The main source of trace metals enrichment of this water mass are the surrounding rivers, whose estuaries are subject to tidal and river discharge dynamics (Ojeda et al., 1995; Díez-Minguito et al., 2012; Garel, 2017). More specifically, while high river discharge rates could export the trace metals onto the inner and middle shelf, low discharge rates would favour their accumulation in the vicinity of the estuary. In both cases, their subsequent advection would depend on the ambient currents (Laiz et al., 2020). In our case, the surface circulation pattern during the STOCA campaign (Fig. 3a) lead to the observed eastward decreasing gradient.

The fluxes calculated within the GoC (Fig. 9) showed a south-eastward transport, with the largest values within the continental shelf (disregarding Mo). This supports the idea that those metals have a terrestrial origin and are transported along the continental shelf, as mentioned above, and in agreement with previous studies (van Geen et al., 1991; Laiz et al., 2020). Furthermore, the largest fluxes of Co, Cu, Fe, and Zn were obtained near the Guadalquivir estuary, implying that this river might be their main source, as also reported by González-Ortegón et al. (2019). In the case of Zn, the largest flux was observed in the two stations closest to the GD estuary, where its concentration was the highest of the whole study (26.52 nM) (Figs. 5f and 8) and in range with previous works (24.50–36.00 nM in van Geen et al., 1991). This could be related to the tidal resuspension of Zn-rich sediments from ancient contamination events (Palanques et al., 1999) or to the paint used in some vessels and ports (e.g., Tovar-Sánchez et al., 2018).

In the case of Cd, Ni, Pb, and Mo, the largest fluxes were obtained within the TF transect, along with an increase in the Cu fluxes (Fig. 9b), probably as a result of terrestrial inputs from the coastal edge (Cd, Ni, Pb) or to the presence of upwelled NACW (Mo, Pb), as indicated by Laiz et al. (2020). Cape Trafalgar is characterised by a quasi-permanent tidally induced upwelling (e.g., Sala et al., 2018) and the presence of a cyclonic gyre to the east of TF that prevents the washout of the upwelled water and favours a high residence time (between 2 and 4 days, Bolado-Penagos et al., 2020; Sala, 2021). This water retention could also be favouring the retention of trace metals inputs from the coastal edge, especially Cu, Cd, Pb, and Mo. The high values of Pb (0.67 nM) observed in the TF transect coastal station (Fig. 5g, Table S1) are in line with previous studies reporting high concentrations (~ 0.30 nM) in the Atlantic inflow of surface water in an area adjacent to the SoG (Morley et al., 1997). On the one hand, this input of Pb could be related to a terrestrial source, as previously observed for the Sicilian Strait by (Morley et al., 1997). On the other hand, it could also be related to aeolian depositions, the upwelling of ancient Pb-rich sediments from burning leaded petrol (Neff, 2002) or to local anthropogenic industrial sources (Desboeufs et al., 2018), as the case of Cu, Cd, and Mo.

5.2. Strait of Gibraltar

Excepting Mo and Ni, the mean concentration values within the SoG (Fig. 8) were half of the ones in the GoC. Considering that the sampling in the SoG was carried out a few days after strong easterly winds (Fig. 2a), the eastward connection between the GoC and the SoG was probably interrupted (see the AJ oriented towards the east-southeast, > 180° in Figs. 2b and 3c, Bolado-Penagos et al., 2020). The presence of easterly winds and the subsequent changes in the AJ could have favoured the induction of turbulence and vertical mixing. Hence, the dilution of metals concentration (Co, Cu, Fe, Cd, Zn) is provoked by mixing the metal-rich surface waters from the GoC with Mediterranean water, which contains a lower metal concentration (Boyle et al., 1985; Tovar-Sánchez et al., 2018). Furthermore, trace metals concentration and their fluxes (Fig. 9) within the SoG presented a tidally induced variation (Fig. S4), showing the lowest/highest values when the tidal current was flowing westward (eastward). The intensity of the trace metal fluxes during eastward flowing currents was twice as much as during westward flowing currents. These results highlight the GoC as the origin of those metals (Boyle et al., 1985; van Geen et al., 1991; Periáñez, 2009; Laiz et al., 2020).

The highest trace metals concentration (Fig. 6) and fluxes (Fig. 9) at the coastal stations and their decreasing gradient towards the centre of the channel might imply an input from the coastal edge. According to Neff (2002), the input of Cu, Cd, Zn, and Pb from the coastal border may be closely related to the pollution from industrial areas (Cu), anthropogenic sources near the coast (Cd), paints from submerged steel surfaces (Zn), or, as explained before, the upwelling of Pb-rich sediments. In addition, previous studies reported aeolian emissions of Co, Cu, Cd, Ni, Zn, Pb, and Mo from oil refineries in the Bay of Algeciras (Fig. 1; Sánchez de la Campa et al., 2011). Finally, agricultural inputs, boat trafficking, and antifoulant biocide for vessels can also contribute to the input of Cu into the ocean (Omanović et al., 2006). The larger fluxes obtained within the SoG in

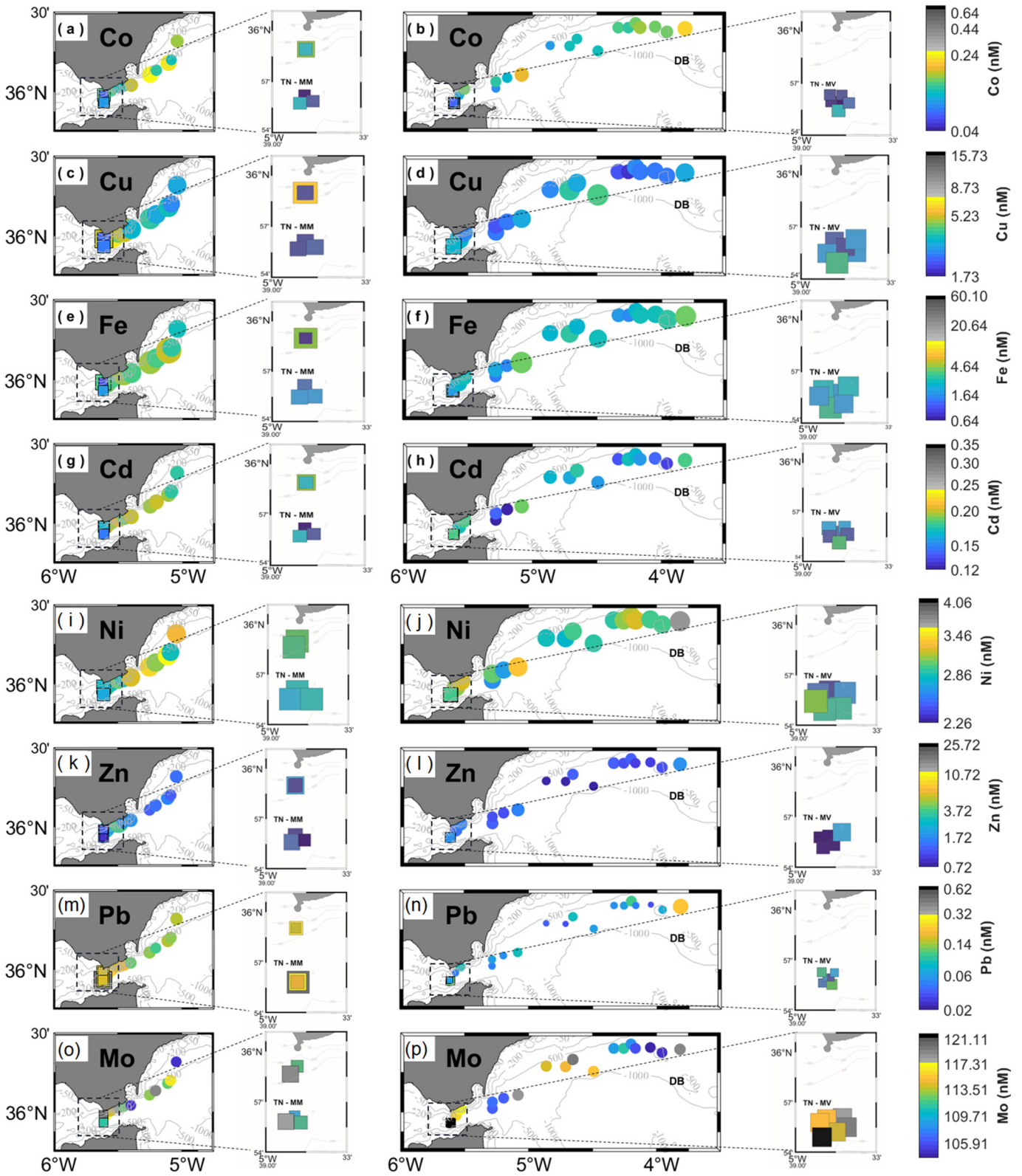

Fig. 6. Trace metals concentration (nM) during the MEGAN TN-NT, TN-VV, LAG1, and LAG2 sampling phases: (a-b) cobalt (Co), (c-d) copper (Cu), (e-f) iron (Fe), (g-h) cadmium (Cd), (i-j) nickel (Ni), (k-l) zinc (Zn), (m-n) lead (Pb), and (o-p) molybdenum (Mo). Left-hand panels show the stations sampled during neap tides at TN-NT (solid squares) and LAG1 (solid circles). Right-hand panels show the stations sampled during spring tides at TN-ST (solid squares) and LAG2 (solid circles). Insets represent a zoom for the TN-NT and TN-ST sampling stations. The size of the circles is proportional to the metal concentration of each metal. Please note the different ranges of scales between subplots. DB: Djibouti Bank.

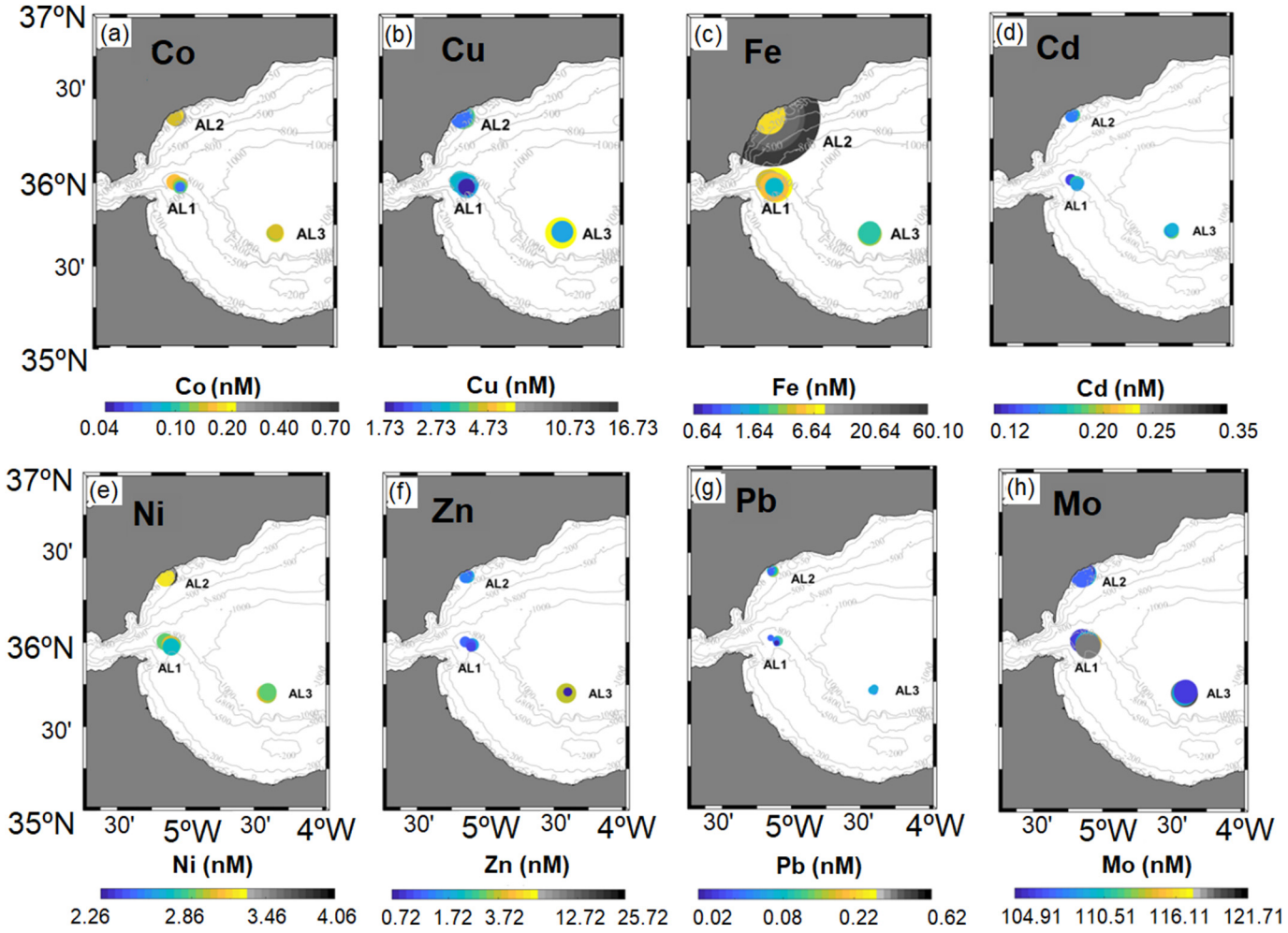

Fig. 7. Trace metals concentration (nM) for the daily cycles in the Alboran Sea stations (AL1, AL2 and AL3). (a) Cobalt (Co), (b) copper (Cu), (c) iron (Fe), (d) cadmium (Cd), (e) nickel (Ni), (f) zinc (Zn), (g) lead (Pb), and (h) molybdenum (Mo). The size of the circles is proportional to the metal concentration of each metal. Please note the different ranges of scales between subplots.

comparison with those in the GoC (Fig. 9c) imply the existence of a local external source.

Apart from anthropogenic sources or the Saharan dust (Tovar-Sánchez et al., 2018), the increase in dissolved Fe concentration in the ocean has also been associated with pyrogenic emissions (Ito et al., 2021). In fact, during 2015 there were 67 forest fires in the region of Cadiz (MAPAMA, 2017), most of which took place in the surroundings of the SoG (San Roque, Tarifa, and Algeciras) at the end of August (López Santalla and López García, 2019), i.e., only one month before the samplings. The dissolution of these pyrogenic particles could have provoked an increase in the surface Fe concentration, as reported in the Mediterranean surface waters in August 2003 (Guieu et al., 2005).

5.3. Alboran Sea

The Lagrangian phases of the MEGAN campaign aimed to analyse the temporal variability of the AJ properties as it moved towards the Alboran Sea. Since the AJ connects the GoC and the Alboran Sea, an eastward decreasing gradient in the trace metals concentration would be expected. This was indeed observed for Cu, Cd, Zn, and Pb. However, the concentrations of Co, Fe, and Ni were larger in the Alboran Sea than in the SoG by a factor of 1.51 nM, 1.67 nM, and 1.08 nM, respectively (Fig. 8).

During neap tides, the highest concentrations of all trace metals, in LAG1 stations, were registered west of the SoG (Fig. 6). According to Bolado-Penagos et al. (2020), the interaction of the AJ with the CsCG could reduce the speed of the jet at this point, leading to a longer residence time of the water masses (~ 3 days), thus allowing the sampling of metal-rich waters that came from the GoC. Nevertheless, the SoG surface waters may also receive inputs from the industrial area of the Bay of Algeciras (Periáñez, 2004), especially in the case of Pb, Fe, Cd, Co, Cu, and Zn which showed concentrations of >1.30 times higher than those observed during spring tides (LAG2). In the days before the spring tides sampling (LAG2), a strong easterly wind event took place (Fig. 2a), interrupting the eastward connection between the GoC and the SoG (Fig. 3c) and disrupting the AJ-WAG system (Fig. 4c) (Bolado-Penagos et al., 2020). Consequently, this event may have also caused an interruption in the expected transport of trace metals from the GoC, which, together with the more intense vertical mixing characteristic of spring tides (Macias et al., 2006), resulted in the lower concentration values obtained compared to the neap tides sampling (Table S1). Nevertheless, the high anomalies observed for Cu, Fe, and Mo at the west of the SoG could be related to the presence of a cyclonic cell that is typically formed at the easternmost exit of the SoG under easterly winds (Soto-Navarro et al., 2016; Chioua et al., 2017; Bolado-Penagos et al., 2021).

The daily cycles sampled in the Alboran Sea allowed us to analyse the offshore gradient in that region. Excepting Mo and Cu, the trace metals' average concentrations (Fig. S1) were at least 1.30 times higher at the Coast (AL2) than at the Jet (AL1) or the Gyre (AL3). This was particularly notable for Fe, whose concentration at the Coast was 5.57 times larger than at the Jet station, and 10.03 times larger than at the Gyre location (Sherrell and Boyle, 1988). According to them, the large Fe concentration

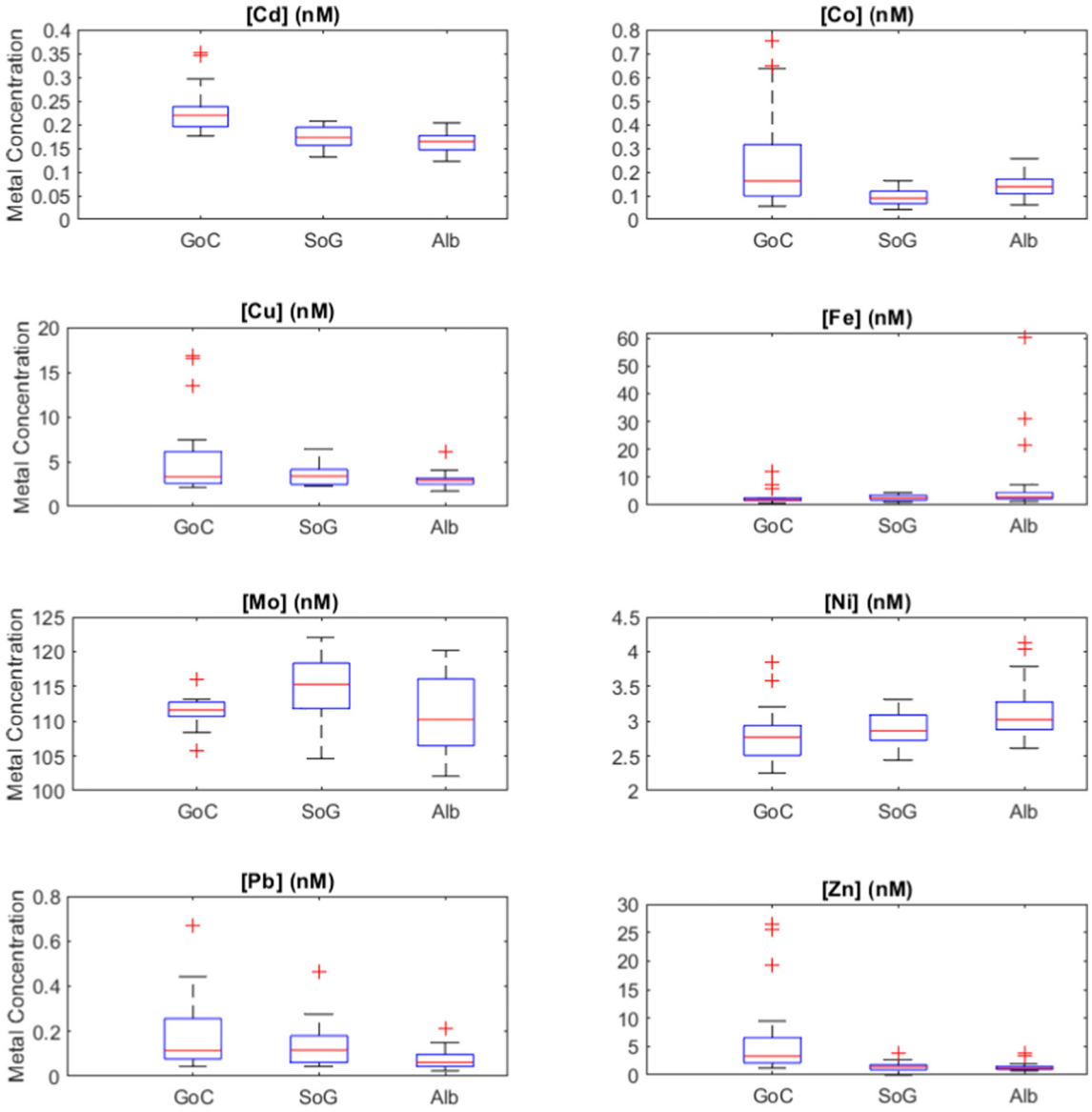

Fig. 8. Boxplot of trace metals concentration (nM) during the whole survey at the three studied regions (GoC: Gulf of Cadiz, SoG: Strait of Gibraltar, Alb: Alboran Sea). (Cadmium (Cd), cobalt (Co), copper (Cu), iron (Fe), molybdenum (Mo), nickel (Ni), lead (Pb) and zinc (Zn).

could come from the dissolution of Fe-rich particles, either by aeolian deposition or by sediment resuspension due to the proximity to a high-energy shelf environment, such as the CsCG. Regarding aeolian inputs, it should be noted that a dust intrusion event from the Sahara Desert took place on 5th October 2015 (Fig. S5), i.e., just one day before the AL* samplings. Moreover, as explained before, the high Fe concentrations could be related to pyrogenetic emissions (Ito et al., 2021; MAPAMA, 2017).

The concentrations of Mo at the Jet were higher than at the Coast, so it did not present the coastal gradient mentioned above (Figs. 7h and 8). Rather, its highest concentration in the whole study was observed in the SoG (Fig. 6p). So, the high value reported at the Jet could be influenced by the advection from the SoG and by the aeolian emissions from petroleum refineries near the Bay of Algeciras (Sánchez de la Campa et al., 2011). Cd and Cu at Jet presented a similar concentration to the coastal station and were also related to the above-mentioned anthropogenic sources (Fig. S1). Nevertheless, the rest of the trace metals concentration at the Jet station remained lower than at the coastal one (Fig. S1). As already mentioned, this could be related to the origin of the sampled water mass, which corresponded to metal-depleted Surface Atlantic Water (Fig. S3b), in agreement with Laiz et al. (2020).

The minimum value of Fe concentration for the whole study was found at the Gyre (AL3) station, which is consistent with the oligotrophic nature of this location (Boyle et al., 1985). However, this station did not show the minimum concentrations in the survey for the rest, but it showed high values of Cu and Zn (Figs. 7b, f, 9). According to previous studies in the same region (Boyle et al., 1985; Sherrell and Boyle, 1988), the accumulation of some trace metals (Cu, Cd, Ni or Zn) in the surface waters may be the result of the low degree of remineralisation and with inefficient scavenging by phytoplankton. Sherrell and Boyle (1988) suggested that the origin of these metals in the Mediterranean surface waters could be related to aeolian contributions (either natural from the Sahara or anthropogenic from polluting sources), as well as fluvial or diagenetic.

6. Conclusions

The distribution of dissolved Co, Cu, Fe, Cd, Ni, Zn, Pb, and Mo along the GoC, SoG and Alboran Sea surface waters was studied with in-situ data. These results complement previous studies on trace metals from the GoC (Boyle et al., 1985; van Geen et al., 1991; Periáñez, 2009; González-Ortegón et al., 2019; Laiz et al., 2020) and, as a novelty, explain changes

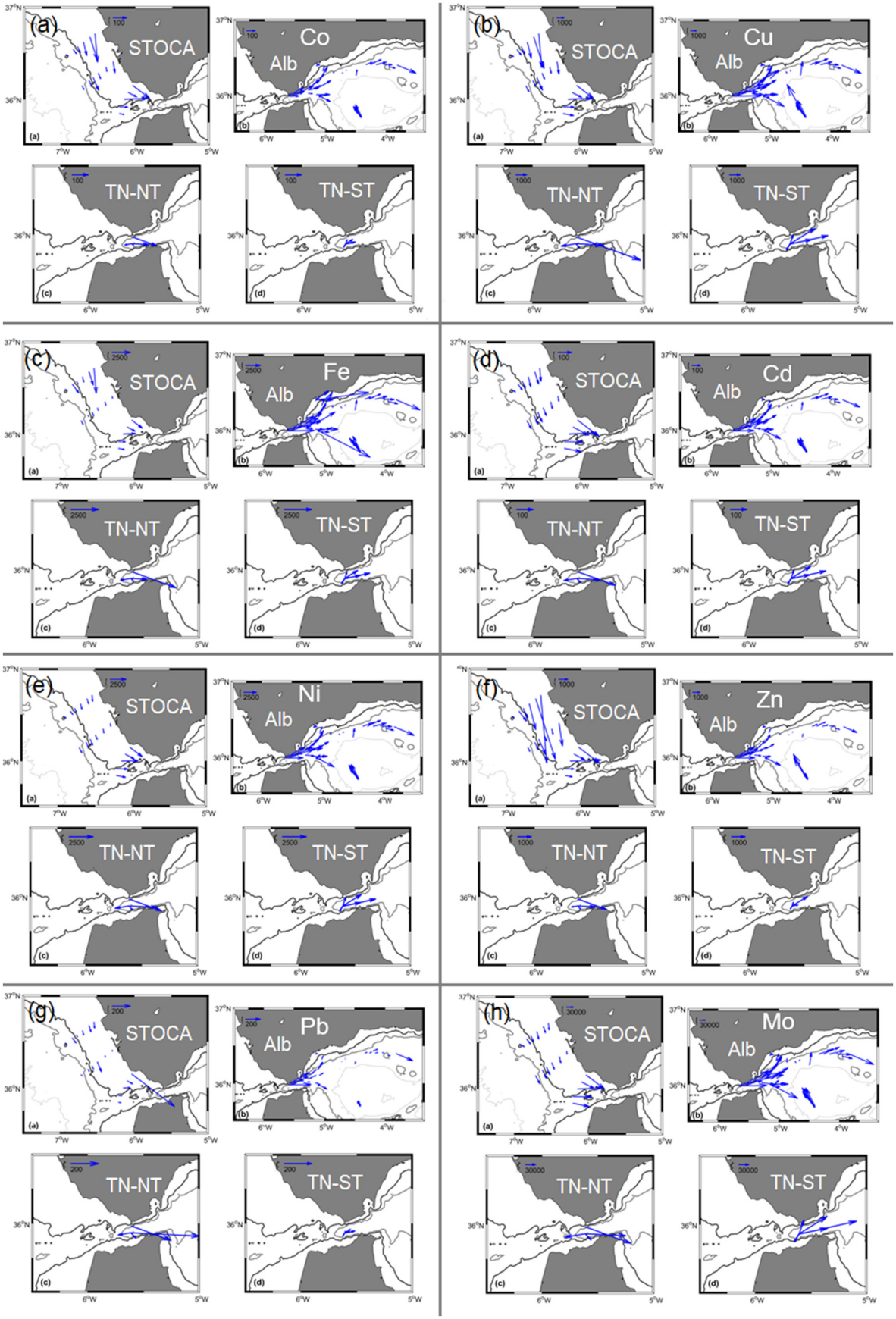

Fig. 9. Horizontal advective fluxes (nmol $m^{-2} s^{-1}$) for (a) Co, (b) Cu, (c) Fe, (d) Cd, (e) Ni, (f) Zn, (g) Pb and (h) Mo. calculated at the STOCA (GD, SP and TF), and MEGAN stations (TN-NT, TN-ST, Alb, the latter including LAG1, LAG2 and AL1, AL2, and AL3). GD: Guadiana, SP: Sancti Petri, TF: Trafalgar, TN: Tarifa Narrow, NT: Neap Tides, ST: Spring Tides, Alb: Alboran Sea.

in the distribution of trace metals as they are advected from the GoC through the SoG.

The analysis of the concentration of trace metals' distribution in the study region showed an eastward gradient from the GoC to the Alboran Sea, and from the coast to the open ocean. However, distribution variability was observed, depending on the metal analysed, related to its specific sources (e.g., Zn or Pb from boats and industrial pollution) and to the influence of different physical processes (e.g., retention of surface water masses).

The hydrodynamic of the area, that connects the origin of most metals (shelf waters of the GoC) with the Alboran Sea, decreased progressively their concentrations, a process that was accelerated by vertical mixing (e.g., wind or tides). This is the case of the dilution of metals concentration (Co, Cu, Fe, Cd, Zn) in the SoG.

However, a concentration increase associated with coastal inputs was also observed in the SoG and the Alboran Sea (e.g., Pb from industrial pollution in the SoG and Fe from pyrogenetic emissions at the coast of the Alboran Sea). This increase coincides with the presence of sub- and mesoscale structures (e.g., the cyclonic gyre near Cape Trafalgar, or the CsCG) that favour the residence time of the water mass (~ 2–4 days and 3 days, respectively). Hence, the surface waters are more exposed to trace metals' input from the coastal edge.

CRediT authorship contribution statement

Mª. Andrea Orihuela-García: Data curation, Formal analysis, Investigation, Software, Visualization, Writing – original draft, Writing – review & editing. **Marina Bolado-Penagos:** Conceptualization, Data curation, Formal analysis, Methodology, Software, Visualization, Writing – original draft, Writing – review & editing. **Iria Sala:** Investigation, Writing – review & editing. **Antonio Tovar-Sánchez:** Conceptualization, Funding acquisition, Project administration, Resources, Supervision, Writing – review & editing. **Carlos M. García:** Conceptualization, Funding acquisition, Project administration, Resources, Supervision, Writing – review & editing. **Miguel Bruno:** Conceptualization, Supervision, Writing – review & editing. **Fidel Echevarría:** Conceptualization, Funding acquisition, Project administration, Resources, Supervision, Writing – review & editing. **Irene Laiz:** Conceptualization, Data curation, Formal analysis, Methodology, Software, Visualization, Writing – original draft, Writing – review & editing.

Data availability

Data will be made available on request.

Declaration of competing interest

The authors declare that they have no known competing financial interests or personal relationships that could have appeared to influence the work reported in this paper.

Acknowledgements

Firstly, we would like to thank the two anonymous reviewers for their thoughtful comments and efforts towards improving our manuscript. The authors gratefully acknowledge the crew and technical staff of the R.V. *Sarmiento de Gamboa* and R.V. *Ángeles Alvariño* for their help during the cruises, and scientific teams of MEGAN and MEGOCA projects. Authors also gratefully acknowledge the Spanish *Puertos del Estado* for the freely available datasets: High-Frequency Radar daily observations and SAMPA numerical simulations that were collected from their Institution's website (http://opendap.puertos.es/), and Copernicus Marine Service for the Chlorophyll-*a* satellite imagery used in this work (OCEANCOLOUR_ATL_CHL_L4_NRT_OBSERVATIONS_009_037). This work has been supported by the Spanish National Research Plan through the projects: CTM2013-49048 (MEGAN), CTM2014-59244-C3-3-R (MEGOCA), and STOCA (*Instituto Español de Oceanografía*). M. Andrea Orihuela-García is supported by a grant from the FPI fellowship program. Marina Bolado-Penagos and Iria Sala were supported by a grant from the FPI fellowship program, in Spain.

Appendix A. Supplementary data

Supplementary data to this article can be found online at https://doi.org/10.1016/j.scitotenv.2022.159662.

References

Beckers, J.M., Achterberg, E.P., Braungardt, C., 2007. Comparison of high spatial resolution trace metal distributions with model simulations for surface waters of the Gulf of Cadiz. Estuar. Coast. Shelf Sci. 74, 599–609. https://doi.org/10.1016/j.ecss.2006.12.020.

Blasco, J., Sáenz, V., Gómez-Parra, A., 2000. Heavy metal fluxes at the sediment-water interface of three coastal ecosystems from south-west of the Iberian Peninsula. Sci. Total Environ. 247, 189–199. https://doi.org/10.1016/S0048-9697(99)00490-8.

Bolado-Penagos, M., González, C.J., Chioua, J., Sala, I., Jesús Gomiz-Pascual, J., Vázquez, Á., Bruno, M., 2020. Submesoscale processes in the coastal margins of the strait of Gibraltar. The trafalgar – alboran connection. Prog. Oceanogr. 181, 102219. https://doi.org/10.1016/j.pocean.2019.102219.

Bolado-Penagos, M., Sala, I., Gomiz-Pascual, J.J., Romero-Cózar, J., González-Fernández, D., Reyes-Pérez, J., Vázquez, A., Bruno, M., 2021. Revising the effects of local and remote atmospheric forcing on the Atlantic jet and Western alboran gyre dynamics. J. Geophys. Res. Ocean. 126, 1–33. https://doi.org/10.1029/2020JC016173.

Bormans, M., Garrett, C., 1989. A simple criterion for gyre formation by the surface outflow from a strait, with application to the alboran sea. J. Geophys. Res. Ocean. 94, 12637–12644. https://doi.org/10.1029/JC094iC09p12637.

Boyle, E.A., Chapnick, S.D., Bai, X.X., Spivack, A., 1985. Trace metal enrichments in the Mediterranean Sea. Earth Planet. Sci. Lett. 74, 405–419. https://doi.org/10.1016/S0012-821X(85)80011-X.

Braungardt, C.B., Achterberg, E.P., Elbaz-Poulichet, F., Morley, N.H., 2003. Metal geochemistry in a mine-polluted estuarine system in Spain. Appl. Geochemistry 18, 1757–1771. https://doi.org/10.1016/S0883-2927(03)00079-9.

Bruno, M., Chioua, J., Romero, J., Vázquez, A., Macías, D., Dastis, C., Ramírez-Romero, E., Echevarria, F., Reyes, J., García, C.M., 2013. The importance of sub-mesoscale processes for the exchange of properties through the strait of Gibraltar. Prog. Oceanogr. 116, 66–79. https://doi.org/10.1016/j.pocean.2013.06.006.

Chioua, J., Ruiz, M.I., Alvarez, E., Dastis, C., Gonz, C.J., Bruno, M., Yanguas, F., Romero, J., Alvarez, O., 2017. Water exchange between Algeciras Bay and the strait of Gibraltar : a study based on HF coastal radar. Estuar. Coast. Shelf Sci. 196, 109–122. https://doi.org/10.1016/j.ecss.2017.06.030.

Cotté-Krief, M.H., Guieu, C., Thomas, A.J., Martin, J.M., 2000. Sources of cd, cu, ni and zn in portuguese coastal waters. Mar. Chem. 71, 199–214. https://doi.org/10.1016/S0304-4203(00)00049-9.

Criado-Aldeanueva, F., García-Lafuente, J., Vargas, J.M., Del Río, J., Vázquez, A., Reul, A., Sánchez, A., 2006. Distribution and circulation of water masses in the Gulf of Cadiz from in situ observations. Deep. Res. Part II Top. Stud. Oceanogr. 53, 1144–1160. https://doi.org/10.1016/j.dsr2.2006.04.012.

Criado-Aldeanueva, F., Garcia-Lafuente, J., Navarro, G., Ruiz, J., 2009. Seasonal and interannual variability of the surface circulation in the eastern gulf of Cadiz (SW Iberia). J. Geophys. Res. Ocean. 114. https://doi.org/10.1029/2008JC005069.

De Oliveira Júnior, L., Garel, E., Relvas, P., 2021. The structure of incipient coastal counter currents in South Portugal as indicator of their forcing agents. J. Mar. Syst. 214, 103486. https://doi.org/10.1016/j.jmarsys.2020.103486.

Desboeufs, K., Bon Nguyen, E., Chevaillier, S., Triquet, S., Dulac, F., 2018. Fluxes and sources of nutrient and trace metal atmospheric deposition in the northwestern Mediterranean. Atmos. Chem. Phys. 18, 14477–14492. https://doi.org/10.5194/acp-18-14477-2018.

Díez-Minguito, M., Baquerizo, A., Ortega-Sánchez, M., Navarro, G., Losada, M.A., 2012. Tide transformation in the Guadalquivir estuary (SW Spain) and process based zonation. J. Geophys. Res. 117, C03019. https://doi.org/10.1029/2011JC007344.

Donázar-Aramendía, I., Sánchez-Moyano, J.E., García-Asencio, I., Miró, J.M., Megina, C., García-Gómez, J.C., 2018. Maintenance dredging impacts on a highly stressed estuary (Guadalquivir estuary): a BACI approach through oligohaline and polyhaline habitats. Mar. Environ. Res. 140, 455–467. https://doi.org/10.1016/j.marenvres.2018.07.012.

Elbaz-Poulichet, F., Morley, N.H., Beckers, J.M., Nomerange, P., 2001. Metal fluxes through the strait of Gibraltar: the influence of the tinto and odiel rivers (sw spain). Mar. Chem. 73, 193–213. https://doi.org/10.1016/S0304-4203(00)00106-7.

Gaillardet, J., Viers, J., Dupré, B., 2014. Trace elements in river waters. Second Edition, Treatise on Geochemistry. https://doi.org/10.1016/B978-0-08-095975-7.00507-6.

García-Lafuente, J., Delgado, J., Criado, F., 2002. Inflow interruption by meteorological forcing in the Strait of Gibraltar 29, 2–5. https://doi.org/10.1029/2002GL015446.

García-Lafuente, J., Delgado, J., Criado-Aldeanueva, F., Bruno, M., del Rio, J., Vargas, J.M., 2006. Water mass circulation on the continental shelf of the Gulf of Cadiz. Deep Sea Res. Part II, 53 (11–13), 1182–1197. https://doi.org/10.1016/j.dsr2.2006.04.011.

Garel, E., 2017. Present dynamics of the guadiana estuary. In: Moura, D., Gomes, A., Mendes, I., Aníbal, J. (Eds.), Guadiana River Estuary – Investigating the Past, Present, and Future, 1st edition University of Algarve, Faro, pp. 15–37. http://hdl.handle.net/10400.1/9887.

Garel, E., Laiz, I., Drago, T., Relvas, P., 2016. Characterisation of coastal counter-currents on the inner shelf of the Gulf of Cadiz. J. Mar. Syst. 155, 19–34. https://doi.org/10.1016/j.jmarsys.2015.11.001.

van Geen, A., Boyle, E., 1990. Variability of trace-metal fluxes through the strait of Gibraltar. Glob. Planet. Change 3, 65–79. https://doi.org/10.1016/0921-8181(90)90056-I.

van Geen, A.Van, Rosener, P., Boyle, E., 1988. Entrainment of trace-metal-enriched Atlantic-Shelf water in the inflow to the Mediterranean Sea 3–6.
van Geen, A., Boyle, E.A., Moore, W.S., 1991. Trace metal enrichments in waters of the Gulf of Cadiz. Spain. Geochim. Cosmochim. Acta 55, 2173–2191. https://doi.org/10.1016/0016-7037(91)90095-M.
Geibert, W., 2018. Processes that regulate trace element distribution in the ocean. Elements 14, 391–396. https://doi.org/10.2138/gselements.14.6.391.
González-Ortegón, E., Laiz, I., Sánchez-Quiles, D., Cobelo-Garcia, A., Tovar-Sánchez, A., 2019. Trace metal characterization and fluxes from the guadiana, tinto-odiel and Guadalquivir estuaries to the Gulf of Cadiz. Sci. Total Environ. 650, 2454–2466. https://doi.org/10.1016/j.scitotenv.2018.09.290.
Guieu, C., Bonnet, S., Wagener, T., Loÿe-Pilot, M.D., 2005. Biomass burning as a source of dissolved iron to the open ocean? Geophys. Res. Lett. 32, 1–5. https://doi.org/10.1029/2005GL022962.
Hatje, V., Lamborg, C.H., Boyle, E.A., 2018. Trace-metal contaminants: human footprint on the ocean. Elements 14, 403–408. https://doi.org/10.2138/gselements.14.6.403.
Henderson, G.M., Anderson, R.F., Adkins, J., Andersson, P., Boyle, E.A., Cutter, G., Baar, H.D., Eisenhauer, A., Frank, M., Francois, R., Orians, K., Gamo, T., German, C., Jenkins, W., Moffett, J., Jeandel, C., Jickells, T., Krishnaswami, S., Mackey, D., 2007. GEOTRACES - an international study of the global marine biogeochemical cycles of trace elements and their isotopes. Chem. Erde 67, 85–131. https://doi.org/10.1016/j.chemer.2007.02.001.
Hierro, A., Olías, M., Cánovas, C.R., Martín, J.E., Bolivar, J.P., 2014. Trace metal partitioning over a tidal cycle in an estuary affected by acid mine drainage (Tinto estuary, SW Spain). Sci. Total Environ. 497–498, 18–28. https://doi.org/10.1016/j.scitotenv.2014.07.070.
Ito, A., Ye, Y., Baldo, C., Shi, Z., 2021. Ocean fertilization by pyrogenic aerosol iron. Npj clim. Atmos. Sci. 4, 1–20. https://doi.org/10.1038/s41612-021-00185-8.
Kidd, P.S., Domínguez-Rodríguez, M.J., Díez, J., Monterroso, C., 2007. Bioavailability and plant accumulation of heavy metals and phosphorus in agricultural soils amended by long-term application of sewage sludge. Chemosphere 66, 1458–1467. https://doi.org/10.1016/j.chemosphere.2006.09.007.
Laiz, I., Plecha, S., Teles-Machado, A., González-Ortegón, E., Sánchez-Quiles, D., Cobelo-García, A., Roque, D., Peliz, A., Sánchez-Leal, R.F., Tovar-Sánchez, A., 2020. The role of the Gulf of Cadiz circulation in the redistribution of trace metals between the Atlantic Ocean and the Mediterranean Sea. Sci. Total Environ. 719. https://doi.org/10.1016/j.scitotenv.2019.134964.
Leistel, J.M., Marcoux, E., Deschamps, Y., 1997. Chert in the iberian Pyrite Belt. Miner. Depos. 33, 59–81. https://doi.org/10.1007/s001260050133.
López Santalla, A., López García, M., 2019. Los incendios forestales en España, decenio 2006–2015. Minist. Agric. pesca y Aliment. 1–140.
Macias, D., García, C.M., Echevarría Navas, F., Vázquez-López-Escobar, A., Bruno Mejías, M., 2006. Tidal induced variability of mixing processes on camarinal sill (Strait of Gibraltar): a pulsating event. J. Mar. Syst. 60, 177–192. https://doi.org/10.1016/j.jmarsys.2005.12.003.
Macías, D., Bruno, M., Echevarría, F., Vázquez, A., García, C.M., 2008. Meteorologically-induced mesoscale variability of the north-western Alboran Sea (southern Spain) and related biological patterns. Estuar. Coast. Shelf Sci. 78, 250–266. https://doi.org/10.1016/j.ecss.2007.12.008.
Macías, D., García-Gorriz, E., Stips, A., 2016. The seasonal cycle of the Atlantic Jet dynamics in the Alboran Sea : direct atmospheric forcing versus. Mediterranean thermohaline circulation, 137–151. https://doi.org/10.1007/s10236-015-0914-y.
MAPAMA, 2017. Incendios forestales en España Año 2015, pp. 1–95.
Mauritzen, C., Morel, Y., Paillet, J., 2001. On the influence of Mediterranean water on the central waters of the North Atlantic Ocean. Deep. Res. Part I Oceanogr. Res. Pap. 48, 347–381. https://doi.org/10.1016/S0967-0637(00)00043-1.
Micó, C., Recatalá, L., Peris, M., Sánchez, J., 2006. Assessing heavy metal sources in agricultural soils of an european Mediterranean area by multivariate analysis. Chemosphere 65, 863–872. https://doi.org/10.1016/j.chemosphere.2006.03.016.
Morel, F.M.M., Price, N.M., 2003. The biogeochemical cycles of trace metals in the oceans. Science 80). 300, 944–947. https://doi.org/10.1126/science.1083545.
Morley, N.H., Burton, J.D., Tankere, S.P.C., Martin, J.M., 1997. Distribution and behaviour of some dissolved trace metals in the western Mediterranean Sea. Deep. Res. Part II Top. Stud. Oceanogr. 44, 675–691. https://doi.org/10.1016/S0967-0645(96)00098-7.
Neff, J.M., 2002. Lead, copper, cadmium, zinc in the ocean. Bioaccumulation in Marine Organisms., 89–189. https://doi.org/10.1016/b978-008043716-3/50010-5.
Nieto, J.M., Sarmiento, A.M., Olías, M., Canovas, C.R., Riba, I., Kalman, J., Delvalls, T.A., 2006. Acid mine drainage pollution in the tinto and odiel rivers (Iberian Pyrite Belt, SW Spain) and bioavailability of the transported metals to the Huelva estuary. Environ. Int. 33, 445–455. https://doi.org/10.1016/j.envint.2006.11.010.
Ojeda, J., Sanchez, E., Fernandez-Palacios, A., Moreira, J.M., 1995. Study of the dynamics of estuarine and coastal waters using remote sensing: the tinto-odiel estuary. SW Spain. J. Coastal Conserv. 1, 109–118. https://doi.org/10.1007/BF02905119.
Olías, M., Cánovas, C.R., Nieto, J.M., Sarmiento, A.M., 2006. Evaluation of the dissolved contaminant load transported by the tinto and odiel rivers (South West Spain). Appl. Geochemistry 21, 1733–1749. https://doi.org/10.1016/j.apgeochem.2006.05.009.
Omanović, D., Kwokal, Ž., Goodwin, A., Lawrence, A., Banks, C.E., Compton, R.G., Komorsky-Lovrić, Š., 2006. Trace metal detection in Šibenik Bay, Croatia: cadmium, lead and copper with anodic stripping voltammetry and manganese via sonoelectrochemistry. A case study. J. Iran. Chem. Soc. 3, 128–139. https://doi.org/10.1007/BF03245940.
Palanques, A., Puig, P., Guillén, J., Querol, X., Alastuey, A., 1999. Zinc contamination in the bottom and suspended sediments of the Guadalquivir estuary after the aznalcollar spill (south-Western Spain). Control of hydrodynamic processes. Sci. Total Environ. 242, 211–220. https://doi.org/10.1016/S0048-9697(99)00391-5.
Periáñez, R., 2004. A particle-tracking model for simulating pollutant dispersion in the strait of Gibraltar. Mar. Pollut. Bull. 49, 613–623. https://doi.org/10.1016/j.marpolbul.2004.04.003.
Periáñez, R., 2009. Environmental modelling in the Gulf of Cadiz: heavy metal distributions in water and sediments. Sci. Total Environ. 407, 3392–3406. https://doi.org/10.1016/j.scitotenv.2009.01.023.
Relvas, P., Barton, E.D., 2002. Mesoscale patterns in the Cape São Vicente (Iberian Peninsula) upwelling region. J. Geophys. Res. Ocean. 107. https://doi.org/10.1029/2000jc000456.
Renault, L., Oguz, T., Pascual, A., Vizoso, G., Tintore, J., 2012. Surface circulation in the Alborán Sea (western Mediterranean) inferred from remotely sensed data. J. Geophys. Res. Ocean. 117, 1–11. https://doi.org/10.1029/2011JC007659.
Reyes, M., 2015. Modelado de Alta resolución Para el estudio de la respuesta oceánica al forzamiento del viento en el estrecho de Gibraltar. University of Cadiz PhD thesis.
Sala, I., 2021. Physical-biological interaction in the strait of Gibraltar: the trafalgar-Alborán connection. University of Cadiz PhD thesis.
Sala, I., Navarro, G., Bolado-Penagos, M., Echevarría, F., García, C.M., 2018. High-chlorophyll-area assessment based on remote sensing observations: the case study of cape trafalgar. Remote Sens. 10. https://doi.org/10.3390/rs10020165.
Sala, I., Bolado-Penagos, M., Bartual, A., Bruno, M., García, C.M., López-Urrutia, Á., González-García, C., Echevarría, F., 2022. A lagrangian approach to the Atlantic jet entering the Mediterranean Sea: physical and biogeochemical characterization. J. Mar. Syst. 226, 103652. https://doi.org/10.1016/j.jmarsys.2021.103652.
Sánchez de la Campa, A.M., Moreno, T., de la Rosa, J., Alastuey, A., Querol, X., 2011. Size distribution and chemical composition of metalliferous stack emissions in the San Roque petroleum refinery complex, southern Spain. J. Hazard. Mater. 190, 713–722. https://doi.org/10.1016/j.jhazmat.2011.03.104.
Sánchez, R.F., Relvas, P., 2003. Spring-summer climatological circulation in the upper layer in the region of Cape St. Vincent. Southwest Portugal. ICES J. Mar. Sci. 60, 1232–1250. https://doi.org/10.1016/S1054-3139(03)00137-1.
Sánchez, R.F., Mason, E., Relvas, P., da Silva, A.J., Peliz, A., 2006. On the inner-shelf circulation in the northern gulf of Cadiz, southern portuguese shelf. Deep Sea Res. Part II, 53 (11–13), 1198–1218. https://doi.org/10.1016/j.dsr2.2006.04.002.
Sarhan, T., García-Lafuente, J., Vargas, M., Vargas, J.M., Plaza, F., 2000. Upwelling mechanisms in the northwestern Alboran Sea. J. Mar. Syst. 317–331.
Sherrell, R.M., Boyle, E.A., 1988. Zinc, chromium, vanadium and iron in the Mediterranean Sea. Deep Sea res. Part a. Oceanogr. Res. Pap. 35, 1319–1334. https://doi.org/10.1016/0198-0149(88)90085-4.
Soto-Navarro, J., Lorente, P., Alvarez, E., Sánchez-Garrido, J.C., García-Lafuente, J., 2016. Surface circulation at the strait of Gibraltar: a combined HF radar and high resolution model study. J. Geophys. Res. Ocean. 121, 2016–2034. https://doi.org/10.1038/175238c0.
Sunda, W.G., 1989. Trace metal interactions with marine phytoplankton. Biol. Oceanogr. 6, 411–442.
Tovar-Sánchez, A., 2012. Sampling approaches for trace element determination in seawater. Compr. Sampl. Sample Prep. 1, 317–334. https://doi.org/10.1016/B978-0-12-381373-2.00017-X.
Tovar-Sánchez, A., Duarte, C.M., Alonso, J.C., Lacorte, S., Tauler, R., Galban-Malagón, C., 2010. Impacts of metals and nutrients released from melting multiyear Arctic Sea ice. J. Geophys. Res. C Ocean. 115. https://doi.org/10.1029/2009JC005685.
Tovar-Sánchez, A., Arrieta, J.M., Duarte, C.M., Sañudo-Wilhelmy, S.A., 2014. Spatial gradients in trace metal concentrations in the surface microlayer of the Mediterranean Sea. Front. Mar. Sci. 1. https://doi.org/10.3389/fmars.2014.00079.
Tovar-Sánchez, A., González-Ortegón, E., Duarte, C.M., 2018. Trace metal partitioning in the top meter of the ocean. Sci. Total Environ. 652, 907–914. https://doi.org/10.1016/j.scitotenv.2018.10.315.
Twining, B.S., Baines, S.B., 2013. The trace metal composition of marine phytoplankton. Annu. Rev. Mar. Sci. 5, 191–215. https://doi.org/10.1146/annurev-marine-121211-172322.
Vargas-Yáñez, M., Plaza, F., García-Lafuente, J., Sarhan, T., Vargas, J.M., Vélez-Belchi, P., 2002. About the seasonal variability of the Alboran Sea circulation 35, 229–248.
Viúdez, A., Pinot, J.-M., Haney, R.L., 1998. On the upper layer circulation in the Alboran Sea. J. Geophys. Res. 103, 53–60.
Zhang, Shengyin, Guo, H., Zhang, Shuncun, Fan, H., Shi, J., 2020. Are oil spills an important source of heavy metal contamination in the Bohai Sea, China? Environ. Sci. Pollut. Res. 27, 3449–3461. https://doi.org/10.1007/s11356-019-06913-1.